Journal of Power Sources 196 (2011) 3894–3899

Contents lists available at ScienceDirect

Journal of Power Sources

journal homepage: www.elsevier.com/locate/jpowsour

Investigation on the charging process of Li_2O_2-based air electrodes in Li–O_2 batteries with organic carbonate electrolytes

Wu Xu[a,*], Vilayanur V. Viswanathan[a], Deyu Wang[a], Silas A. Towne[a], Jie Xiao[a], Zimin Nie[a], Dehong Hu[b], Ji-Guang Zhang[a,**]

[a] Energy and Environment Directorate, Pacific Northwest National Laboratory, Richland, WA 99354, USA
[b] Fundamental and Computational Sciences Directorate, Pacific Northwest National Laboratory, Richland, WA 99354, USA

ARTICLE INFO

Article history:
Received 15 October 2010
Received in revised form
15 December 2010
Accepted 16 December 2010
Available online 25 December 2010

Keywords:
Li–O_2 battery
Li_2O_2 electrode
Gas chromatography/mass spectroscopy technique
Charging process
Gas evolution
Carbonate electrolyte

ABSTRACT

The charging process of Li_2O_2-based air electrodes in Li–O_2 batteries with organic carbonate electrolytes was investigated using *in situ* gas chromatography/mass spectroscopy (GC/MS) to analyze gas evolution. A mixture of Li_2O_2/Fe_3O_4/Super P carbon/polyvinylidene fluoride (PVDF) was used as the starting air electrode material, and 1-M lithium bis(trifluoromethylsulfonyl)imide (LiTFSI) in carbonate-based solvents was used as the electrolyte. We found that Li_2O_2 was actively reactive to 1-methyl-2-pyrrolidinone and PVDF that were used to prepare the electrode. During the first charging (up to 4.6 V), O_2 was the main component in the gases released. The amount of O_2 measured by GC/MS was consistent with the amount of Li_2O_2 that decomposed during the electrochemical process as measured by the charge capacity, which is indicative of the good chargeability of Li_2O_2. However, after the cell was discharged to 2.0 V in an O_2 atmosphere and then recharged to ~4.6 V, CO_2 was dominant in the released gases. Further analysis of the discharged air electrodes by X-ray diffraction (XRD) and Fourier transform infrared (FTIR) spectroscopy indicated that lithium-containing carbonate species (lithium alkyl carbonates and/or Li_2CO_3) were the main discharge products. Therefore, compatible electrolytes and electrodes, as well as the electrode-preparation procedures, need to be developed for rechargeable Li-air batteries for long term operation.

1. Introduction

Li-air batteries have been widely investigated in recent years because of their ultra-high specific energies, which is a desirable characteristic for a variety of applications including electric vehicles. The theoretical specific energy of a non-aqueous Li-air battery is approximately 11 kWh kg^{-1} based on the lithium electrode alone, and about 5.2 kWh kg^{-1} when the oxygen weight also is included [1,2]. Zheng et al. [3] developed a model to predict the gravimetric and volumetric energy densities of Li-air batteries, and they reported that, for an air electrode with a porosity of 70%, the energy densities of the cell (including Li metal, an organic electrolyte, and carbon) were about 2790 Wh kg^{-1} and 2800 Wh L^{-1}, respectively. Hence, the chemistry of the Li–O_2 battery is an attractive choice for high-energy-density applications. However, the cycle life of a non-aqueous Li–O_2 battery still is not satisfactory, with a cycle life ranging from several cycles to 100 cycles depending on the catalysts and electrolytes used [4–10]. In 2006, Bruce and co-workers [6] reported that a rechargeable Li–O_2 battery using a carbonate-based electrolyte and containing a super S carbon electrode with electrolytic MnO_2 as the catalyst had an initial discharge capacity of 1000 mAh g^{-1} (based on the weight of carbon) at a current rate of 70 mA g^{-1} and a capacity retention of 60% after 50 cycles. They also reported that Li_2O_2 could be charged and significant O_2 evolution was observed when the voltage above 4.5 V. Mizuno et al. [10] reported very recently that a Super P (SP) carbon electrode with MnO_2 powder as a catalyst in a propylene carbonate (PC) electrolyte had an initial discharge capacity of 820 mAh g^{-1} and a 60% capacity retention after 100 cycles, which is the longest cycle life reported for a rechargeable Li–O_2 battery to date. The poor cycle life of the Li–O_2 batteries using carbonate-based electrolytes is probably because the discharge products are mainly carbonates (lithium alkyl carbonates and/or Li_2CO_3) instead of the desired Li_2O_2 [10]. The formation of carbonate products is hypothesized because of the reaction of Li_2O_2 with the PC solvent or with CO_2 gas in the presence of trace moisture, or the decomposition of the PC solvent through reaction with the O_2 radicals or superoxide anions that are formed during the initial O_2 reduction. The discharge products of carbonate species have been confirmed by FTIR spectroscopy spectra [10]; however, the stability of the air electrode and the mechanism of

* Corresponding author. Tel.: +1 509 375 6934; fax: +1 509 375 3864.
** Corresponding author. Tel.: +1 509 372 6515; fax: +1 509 375 3864.
E-mail addresses: wu.xu@pnl.gov (W. Xu), jiguang.zhang@pnl.gov (J.-G. Zhang).

0378-7753/$ – see front matter © 2011 Elsevier B.V. All rights reserved.
doi:10.1016/j.jpowsour.2010.12.065

charge/discharge processes in Li–O_2 batteries still are not well understood.

In this paper, we report on the use of *in situ* GC/MS to investigate gas evolution during the charging processes of a Li–O_2 battery with a Li_2O_2-based electrode and an organic carbonate electrolyte. The components of the reaction products in the air electrodes after charge and discharge were analyzed by XRD and FTIR spectroscopy, and also are discussed.

2. Experimental

2.1. Assembly and test of Li–O_2 coin cells

Li_2O_2 (technical grade, 90%), Fe_3O_4 (nanopowder, <50-nm particle size, ≥98% trace metal basis), 1-methyl-2-pyrrolidinone (NMP, spectrophotometric grade, 99+%), and 4 Å molecular sieves were ordered from Sigma–Aldrich. Lithium foil (99.9%, 0.75 mm thick) was purchased from Alfa Aesar. SP carbon black (from Timcal) and polyvinylidene fluoride (PVDF, from Arkema) were provided by the manufacturers at no charge. A nickel (Ni) foam sheet (density 380 g m^{-2} and thickness 1.7 mm) was obtained from INCO Special Products. LiTFSI, ethylene carbonate (EC), PC, and dimethyl carbonate (DMC) (all battery grade) were purchased from Novolyte Technologies. NMP was dried with excessive 4 Å molecular sieves for a week before use, prior to that the molecular sieves were dried at 300 °C overnight. All other chemicals were used as received.

The Li_2O_2-based air electrodes were prepared as described below inside an MBraun glove box filled with ultra-high purified argon. First, Li_2O_2, Fe_3O_4 (as catalyst), SP, and PVDF at a weight ratio of 36.8:8.7:48.0:6.5 were mixed using two processing methods—one by hand-milling with a marble mortar for 30 min and another by high energy ball-milling on a Spex SamplePrep 8000 M Mixer/Mill for 30 min. Then, slurries of the two mixtures in NMP solvent were separately made and coated onto Ni foam disks with a diameter of 1.59 cm and a flat area of 1.98 cm^2. After the solvent NMP was evaporated in the antechamber of the glove box under vacuum, the air electrodes were further dried at 80 °C under vacuum overnight.

The coin-cell-type Li–O_2 batteries of 2325 size were assembled as described in our previous paper [1]. The 2325 coin cell kits were purchased from Canada National Research Council (CNRC), and 19 mm × ϕ1.0 mm holes were machine-drilled in the cell pans in an evenly distributed pattern so air could pass through. The cells were constructed by (1) placing a Li_2O_2/Fe_3O_4/SP/PVDF/Ni electrode disk on the cell pan with a piece of separator (diameter 2.06 cm, Whatman® GF/D glass microfiber filter paper) placed on the air electrode, (2) adding 280 μL of electrolyte (1.0 M LiTFSI in PC–EC at 1:1 weight ratio) onto the separator, (3) placing a piece of lithium disk, (4) placing a stainless steel spacer with a thickness of 0.5 mm from Pred Materials, and (5) finishing with a coin cell cover with a polypropylene gasket. The whole assembly was crimped inside the glove box on a pneumatic coin cell crimper purchased from CNRC at a gas pressure of 200 psi, and excessive electrolyte was expelled from the cells through the O_2 diffusion holes during crimping.

To examine the electrode processing effect on the performance, Li_2O_2-based air electrodes prepared with and without ball-milling were tested. Each cell was placed in a 226-cm^3 Teflon container, and the container was sealed tightly, with all processes handled inside the argon-filled glove box. The Teflon container with the cell was removed from the glove box and connected to an Arbin BT-2000 battery tester. The cells were charged from the open circuit voltage (OCV) to 4.6 V at a constant current of 70 mA g^{-1} or 40 mA g^{-1} based on the weight of Li_2O_2 on the electrode. The current density varied from 0.11 to 0.35 mA cm^{-2} depending on the weight of Li_2O_2 loaded.

The cell for gas evolution analysis also was placed in the 226-cm^3 Teflon container. After the container was sealed tightly and removed from the glove box, it was connected to a GC/MS instrument. The Teflon container was evacuated and refilled with purified helium at a flow rate of 50 cm^3 min^{-1}. The evacuation and refilling cycle was conducted three times, followed by purging the container with helium for 3.5 h at a flow rate of 3 cm^3 min^{-1}. The cell was charged from the OCV to 4.6 V at a constant current of 70 mA (g^{-1} of Li_2O_2) on a CHI 660C electrochemical analyzer. The gases generated were analyzed in real time using GC/MS (see detailed procedures below). After the charge was completed, the helium gas was switched to O_2 gas. The charged Li–O_2 battery was kept in an O_2 atmosphere of 1.5 atm (i.e., 22 psi) for 2 h to allow the O_2 to diffuse into the cell and equilibrate, and then discharged to 2.0 V at the same current rate (i.e., 70 mA (g^{-1} of Li_2O_2). The O_2 gas in the Teflon container was purged with helium gas for 24 h until the O_2 content was less than 800 ppm. Subsequently, the cell was recharged under the same conditions used in the first charge process, and the gases released during this stage were analyzed.

To investigate the air electrodes after charging and discharging, other Li–O_2 coin cells were assembled and cycled between 4.6 V and 2.0 V in Teflon containers filled with purified O_2. The charge/discharge performance was tested on the Arbin BT-2000 battery tester. Cells were cycled to various states prior to post-mortem analysis: (1) fully charged state after the first cycle, (2) fully discharge state after the first cycle, (3) fully charged state after the second cycle, and (4) fully discharged stage after the second cycle. After the cells were disassembled inside the glove box filled with high-purity argon, the air electrodes were washed thoroughly several times by immersion in fresh anhydrous DMC for at least 1 h each time, followed by drying under vacuum at room temperature overnight.

2.2. GC/MS test

Real-time analysis of gases released from the Li–O_2 battery during the charging processes was conducted using *in situ* GC/MS with helium as the carrier gas. The mass-spectroscopy measurements were made using an SRS RGA 200 instrument with an electron energy of 70 eV and a focus voltage of 90 V. The gas-chromatography measurements were conducted using a two-column Agilent 3000A Micro GC instrument. The injector temperature was 60 °C, with the first column at a temperature of 120 °C and the second column at 40 °C. The concentrations of O_2, nitrogen (N_2), and carbon monoxide (CO) were measured in the first column, and CO_2 concentrations were measured in the second column. Calibration was carried out using 10, 100 and 200 ppm gas standards in helium or N_2 carrier gas. The pressure of the Teflon container housing the coin cells was maintained at 17 psi during charge using a backflow regulator to minimize leaks into the container. For the mass-spectrometry data, a linear fit was done for gas concentration as a function of partial pressure of various gases. For the gas-chromatography data, a linear fit was done for gas concentration vs. both peak area and peak height. Fig. 1 shows the schematic setup of the GC/MS test. A flow rate of 3 cm^3 min^{-1} of the carrier gas was used, and the exit gas from the mass spectrometer was fed into the gas chromatograph. Data from both instruments were in good agreement. Hence, for all runs, the mass spectrometer readings were used.

2.3. Characterizations

XRD measurements of the air electrodes were made on a Philips Xpert X-ray diffractometer with Cu Kα radiation at λ 1.54 Å, from 10° to 80° at a scanning rate of 0.02° per 10 s. The FTIR spectra of the air electrodes were measured on a Bruker Optics Vertex 70

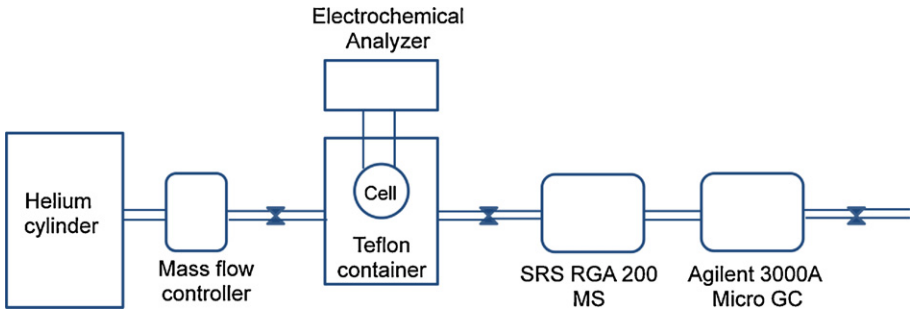

Fig. 1. Schematic setup of the *in situ* GC/MS measurement of gas compositions during Li–O_2 cell charging processes.

FTIR spectrometer with an infrared source from Globar and a KBr beam splitter for the interferometer. The diffuse reflection mode for solid samples was used for all FTIR tests. The sample cell was a Praying Mantis Diffuse Reflection Accessory from Harrick Scientific Products. Because the electrode materials were inside the Ni foam disks, it was difficult to remove them from the Ni foam; therefore, it was not possible to use standard methods for the XRD (in powder) and FTIR (in pellets with KBr) measurements. Therefore, the electrode materials on the Ni foam disks were directly analyzed for XRD and FTIR information.

3. Results and discussion

Fig. 2 shows the comparison of charge profiles of the Li–O_2 cells containing Li_2O_2/Fe_3O_4/SP/PVDF electrodes using two different processing methods and at two different current rates, and 1-M LiTFSI in a PC–EC electrolyte during the first cycle. The charge profile of these cells is quite similar to that reported by Bruce and coworkers [7]. The large overvoltage for the non-ball-milled electrode (the dotted line) shown in Fig. 2 can be attributed to the large Li_2O_2 particle size. After ball milling, the overvoltage was largely reduced as shown in the solid line and the dashed line (see Fig. 2). Without ball milling, the particles of Li_2O_2, Fe_3O_4, and the conductive carbon were larger in size, with poor electrical contact among the particles, resulting in high cell internal resistance. This led to a high overvoltage during charging. On the other hand, high-energy ball milling resulted in smaller particle size, with improved inter-particle electrical contact, which led to a lower overvoltage during the charging process. Lowering the charge current by 43% did not affect the charge voltage significantly (the dashed line in Fig. 2), thus demonstrating that electrode processing was significantly more important than charge current in the determination of overvoltage during charge.

The charge capacity of the Li_2O_2-based air electrodes was nearly independent of processing technique. All three electrodes led to a charge capacity of about 1000 mAh g^{-1} based on Li_2O_2. Taking into consideration of the 90% purity of the Li_2O_2 used in this work, a capacity of 1111 mAh g^{-1} was achieved based on pure Li_2O_2, whose theoretical specific capacity is 1168 mAh g^{-1}. Thus, a 95.1% utilization of Li_2O_2 during charging was obtained.

Fig. 3 shows the composition variations of different gases (helium is not included here) over time during the first charging process for the as-prepared Li_2O_2/Fe_3O_4/SP/PVDF electrode with ball milling in a Li–O_2 cell, along with the charge voltage curve, where a vertical dotted line is plotted to indicate when the charging process started. When charging began, the cell voltage promptly (i.e., within a few minutes) increased to about 4.1 V and then decreased to and stayed at about 4.0 V. We also observed a rapid increase in the O_2 composition, indicating a continual release of O_2 from the decomposition of Li_2O_2. The O_2 concentration increased almost linearly during the first 4 h of charging and then leveled off at 0.24% by volume in the mixed gases. During this time period, there was a small increase in CO_2, CO, and moisture concentrations. Oxygen concentration decreased slightly as the charge voltage approached 4.2 V, accompanied by an obvious increase in the CO_2 and CO concentrations. The evolution of CO_2 and CO was probably resulted from the decomposition of electrolyte solvents (EC and PC) on the high surface area electrode at high voltage (>4.2 V). It

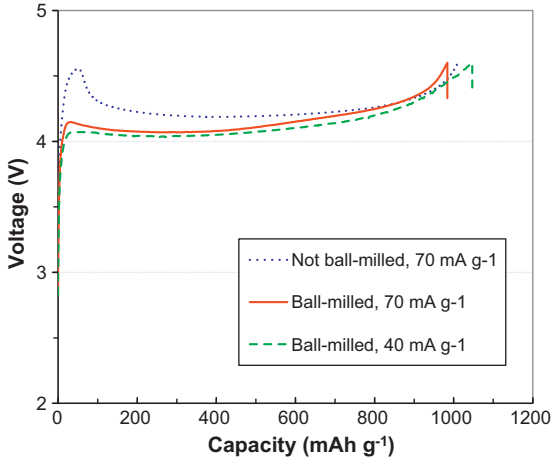

Fig. 2. First cycle charge profiles of Li_2O_2/Fe_3O_4/SP/PVDF electrodes prepared using different approaches and at different current rates.

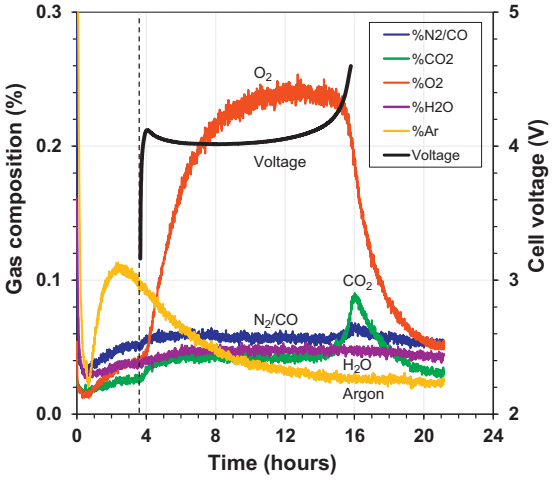

Fig. 3. Variations of charge voltage and gas compositions (helium not included) during the first charging process for the Li_2O_2/Fe_3O_4/SP/PVDF electrode in a carbonate electrolyte.

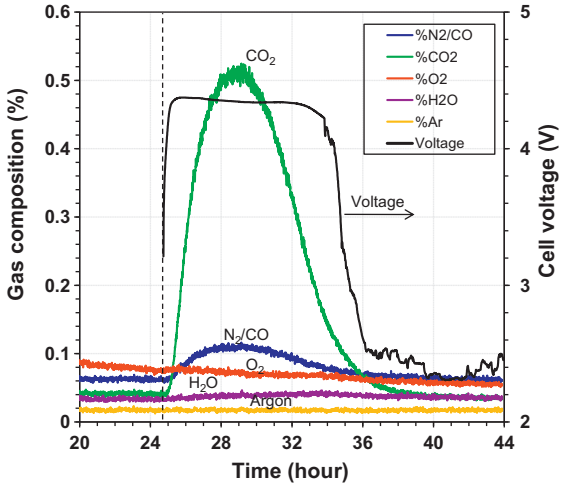

Fig. 4. Variations of charge voltage and gas compositions during the second charging process for Fe_3O_4-based electrode after the first charging and discharging.

should be noted that the composition of N_2 and CO was not separated in our current work, but this will not affect the qualitative analysis of the change in CO concentration during the charging processes.

After the charged cell was discharged to 2.0 V in pure O_2, it was purged with helium and then recharged to the set cutoff voltage of 4.6 V. Fig. 4 shows the variations of cell voltage and gas compositions over time during the second charging process, where a vertical dotted line is plotted to indicate when the charging process began. A quite different phenomenon was observed for this test when compared with that occurring during the first charging process as shown in Fig. 3. The cell voltage increased rapidly to about 4.3 V during the first 30 min of charging. After reaching the maximum voltage at about 4.4 V, a decreasing trend and a sharp decrease in voltage after 10 h charging were observed, and the cutoff voltage of 4.6 V was not achieved. We tested several cells under the same conditions and also at different current rates. All cells showed similar phenomenon during the second charging process in a helium atmosphere. We also found that, if such an air electrode was charged and discharged in an O_2 atmosphere, there was no such voltage drop during the second charging process. It appears that the air electrode would be damaged at voltages that were too high and in an inert atmosphere. The reasons for these phenomena are under investigation. Further cycling of this Li_2O_2-based electrode was not conducted after two cycles because of its poor rechargeability.

Unlike the first charging process for the electrode containing Li_2O_2, the second charging process led to a sharp increase in CO_2 concentration from about 0.04% to about 0.52% within 5 h of charge. There also was an obvious increase in CO concentration and a negligible increase in moisture and O_2 content in the mixed gases. After 5 h of charging, both CO_2 and CO concentrations decreased. Negligible O_2 release during the second charging of the electrode indicates that there is nearly no, or a very limited amount of, Li_2O_2 formed during the prior discharging process, and the materials on the electrodes at the beginning of the first and second charge are quite different. Generation of a significant amount of CO_2 and CO gases during the second charge also indicates that the discharged products are dominated by carbonate species such as lithium alkyl carbonate and/or Li_2CO_3.

Figs. 5A and 6 show the XRD patterns and the FTIR spectra (measured using the diffuse reflection mode), respectively, of the air electrodes in its prepared form (a) where the asterisk (*) indicates the XRD peaks of Li_2O_2 pattern (P01-074-0115), after the first

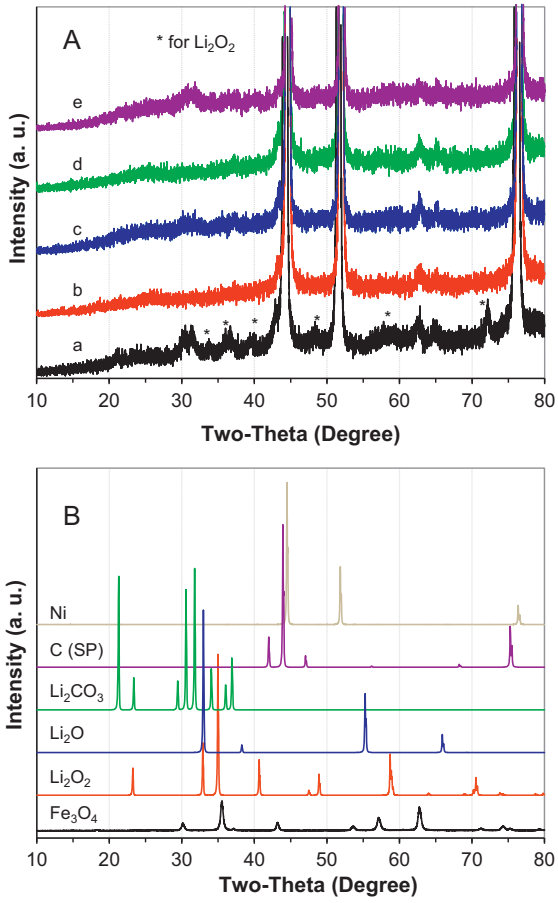

Fig. 5. (A) XRD patterns of the Fe_3O_4-based air electrode in its as-prepared form (a), first charging to 4.6 V (b), first discharging to 2.0 V (c), second charging to 4.6 V (d), and second discharging to 2.0 V (e). The three strong peaks are ascribed to Ni foam used to support the electrode materials. (B) XRD patterns of some standard materials used in this work.

charge to 4.6 V (b), after the first discharge to 2.0 V (c), after the second charge to 4.6 V (d), and after the second discharge to 2.0 V (e). Fig. 5B shows the XRD patterns for some of the standard materials used in this work. The three strong peaks shown in Fig. 5A are ascribed to the Ni foam used to support the electrode materials. Comparing the peaks in Fig. 5A and B, it is interesting to note that both Li_2O_2, which is intentionally used in the initial electrode, and Li_2CO_3, which is not intentionally used in the initial electrode, exist in the as prepared electrode. The formation of Li_2CO_3 in the initial electrode is mainly related to the preparation procedure. During the preparation of the air electrode (Li_2O_2/Fe_3O_4/SP/PVDF), the addition of Li_2O_2 into NMP solvent and PVDF-NMP solution led to rapid color changes. The solution changed from colorless to gray when Li_2O_2 was added to NMP solvent. The solution changed from light yellow to brown when Li_2O_2 was added to the PVDF-NMP solution, while the latter even formed a dark gel when stored for a longer time. We believe that Li_2O_2, which is a strong Lewis base, may react with the NMP solvent and also may lead to PVDF crosslinking. Some carbonate species will form when an air electrode is prepared from an NMP slurry. The FTIR spectrum in Fig. 6a also shows a very small amount of C=O stretch vibration at ca. 1676 cm^{-1}, $RCOO^-$ stretch vibration at 1393 cm^{-1}, and C–O stretch vibration at 1057 cm^{-1}.

After the first charging, the electrode shows XRD patterns for Ni and Fe_3O_4 only (Fig. 5A-b), but the FTIR spectrum shows some small peaks at about 1450 cm^{-1} and 1204 cm^{-1} (Fig. 6b), which correspond to the stretch vibrations of RCOO– and C–O, respectively.

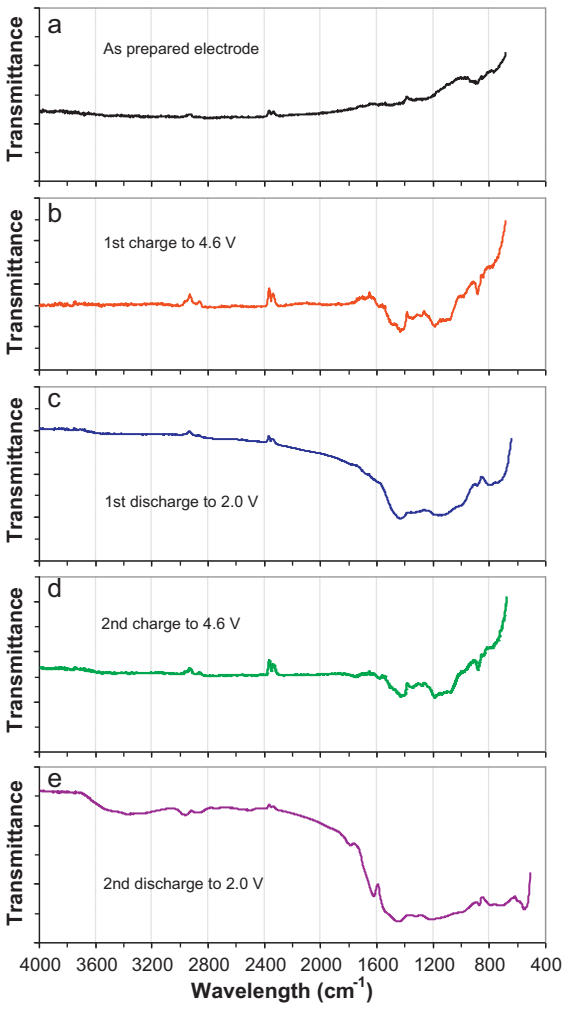

Fig. 6. FTIR spectra in diffusion reflection mode of the Fe_3O_4-based air electrode in its as-prepared form (a), first charging to 4.6 V (b), first discharging to 2.0 V (c), second charging to 4.6 V (d), and second discharging to 2.0 V (e).

The presence of these functional groups probably results from the oxidation of some organic solvents and/or the PVDF binder during the charge process.

When the electrode was discharged to 2.0 V, it did show slight XRD peaks for carbonate (Fig. 5A-c), but no visible peaks of Li_2O_2 or Li_2O were observed. The FTIR spectra in Fig. 6c also shows strong infrared peaks of a $RCOO^-$ stretch vibration at 1479 cm^{-1} and a C–O stretch vibration at 1209 cm^{-1}. These carbonate species are most likely lithium alkylcaronates (such as lithium ethylene dicarbonate and lithium propylene dicarbonate) and are probably formed by the decomposition of carbonate solvents such as PC and EC in the electrolyte used in this work. Aurbach et al. [11–13], Tarasconet al. [14], and Xu et al. [15] confirmed the formation of lithium alkyl mono- and di-carbonates as the essential passivating components in the solid electrolyte interface layer on graphitic carbonaceous materials in lithium-ion batteries containing both cyclic and linear carbonate ester solvents.

After the second charging, the electrode shows nearly the same XRD patterns and FTIR spectra as those shown after the first charging (compare Fig. 5A-d with Fig. 5A-b, and Fig. 6d with Fig. 6b). That is, the XRD curves shown in Fig. 5A-d do not show peaks for Li_2O_2 or Li_2CO_3, while the FTIR spectrum in Fig. 6d still shows small peaks for the $RCOO^-$ stretch vibration at 1479 cm^{-1} and the C–O stretch vibration at 1209 cm^{-1}. This is probably because the carbonate species (lithium alkylcarbonate and/or Li_2CO_3) generated during the first discharging process has not been completely decomposed during the second charging process.

After the second discharging cycle, the electrode shows very similar XRD patterns and FTIR spectra as those shown after the first discharging cycle (compare Fig. 5A-e with Fig. 5A-c, and Fig. 6e with Fig. 6c) but has two extra peaks at 1811 cm^{-1} and 1636 cm^{-1} in the FTIR spectrum corresponding to C=O stretch vibration, respectively.

These results indicate that Li_2O_2 can be charged at a high efficiency; however, discharge in a carbonate-based electrolyte leads to the formation of carbonate species (most likely alkylcarbonate and/or Li_2CO_3), thus causing the irreversible loss of electrolyte and poor rechargeability of the batteries. Therefore, to significantly improve the rechargeability of Li–O_2 or Li-air batteries, it will be necessary to develop new electrolytes (including solvents and salts), electrode materials (including binders and catalysts) and new preparation procedures, all of which are stable towards Li_2O_2 and stable under the charge–discharge voltage range.

4. Conclusions

An *in situ* GC/MS test method has been developed to measure real-time gas evolution during the charging processes of Li–O_2 cells. We have demonstrated that Li_2O_2 can be charged to release O_2 with a high conversion yield. However, the discharged products of the air electrode in a carbonate-based electrolyte are mainly carbonate species, and almost no Li_2O_2 is produced. This finding is consistent with the decomposition of carbonate electrolytes during discharge, and is probably the main reason for the poor cycleability of the Li–O_2 batteries with carbonate electrolytes. We also have found that air electrode processing has large effect on the overvoltage during charging process, and the air electrodes may be damaged when charged to voltages that are too high. Therefore, new electrolytes, electrodes (including materials and processing), and catalysts that are stable during both the charging and discharging processes are required for long-term operation of rechargeable Li–O_2 or Li-air batteries. The solvents used in the electrode-preparation process also need to be carefully selected to avoid possible side reactions during operation of Li-air batteries.

Acknowledgements

This work was conducted under the Laboratory Directed Research and Development Program at Pacific Northwest National Laboratory (PNNL), a multi-program national laboratory operated by Battelle for the U.S. Department of Energy. The authors thank Drs. Jun Liu, Gordon L. Graff, and Mark E. Gross of PNNL for their support and help on the project.

References

[1] W. Xu, J. Xiao, D. Wang, J. Zhang, J.-G. Zhang, J. Electrochem. Soc. 157 (2010) A219.
[2] C.O. Laoire, S. Mukerjee, K.M. Abraham, E.J. Plichta, M.A. Hendrickson, J. Phys. Chem. C 113 (2009) 20127.
[3] J.P. Zheng, R.Y. Liang, M. Hendrickson, E.J. Plichta, J. Electrochem. Soc. 155 (2008) A432.
[4] K.M. Abraham, Z. Jiang, J. Electrochem. Soc. 143 (1996) 1.
[5] J. Read, J. Electrochem. Soc. 149 (2002) A1190.
[6] T. Ogasawara, A. Débart, M. Holzapfel, P. Novák, P.G. Bruce, J. Am. Chem. Soc. 128 (2006) 1390.
[7] A. Débart, J. Bao, G. Armstrong, P.G. Bruce, J. Power Sources 174 (2007) 1177.
[8] A. Débart, A.J. Paterson, J. Bao, P.G. Bruce, Angew. Chem. Int. Ed. 47 (2008) 4521.
[9] H. Cheng, K. Scott, J. Power Sources 195 (2010) 1370.
[10] F. Mizuno, S. Nakanishi, Y. Lotani, S. Yokoishi, H. Iba, Electrochemistry 78 (2010) 403.
[11] D. Aurbach, M.L. Daroux, P.W. Faguy, E. Yeager, J. Electrochem. Soc. 134 (1987) 1611.

[12] D. Aurbach, Y. Gofer, M. Ben-Zion, P. Aped, J. Electroanal. Chem. 339 (1992) 451.
[13] D. Aurbach, Y. Ein-Eli, B. Markovsky, A. Zaban, S. Luski, Y. Carmeli, H. Yamin, J. Electrochem. Soc. 142 (1995) 2822.
[14] L. Gireaud, S. Grugeon, S. Laruelle, S. Pillard, J.-M. Tarascon, J. Electrochem. Soc. 152 (2005) A850.
[15] K. Xu, G.V. Zhuang, J.L. Allen, U. Lee, S.S. Zhang, P.N. Ross Jr., T.R. Jow, J. Phys. Chem. B 110 (2006) 7708.